Wang Mu-xin, Liu Pei-jin*, Yang Wen-jing and Wei Xiang-geng

Nozzle Admittance and Damping Analysis Using the LEE Method

DOI 10.1515/tjj-2015-0050
Received September 8, 2015; accepted October 12, 2015

Abstract: The nozzle admittance is very important in the theoretical analysis of nozzle damping in combustion instability. The linearized Euler equations (LEE) are used to determine the nozzle admittance with consideration of the mean flow properties. The acoustic energy flux through the nozzle is calculated to evaluate the nozzle damping upon longitudinal oscillation modes. Then the parametric study, involving the nozzle convergent geometry, convergent half angle and nozzle size, is carried out. It is shown that the imaginary part of the nozzle admittance plays a non-negligible role in the determination of the nozzle damping. Under the conditions considered in this work (f^* = 1,000 Hz, de^* = 0.18 m), the acoustic energy flux released from the nozzle with a 30° convergent half angle is highest (30°:6.0×10^4kgs^{-3}, 45°:5.2×10^4kgs^{-3}, 60°:4.9×10^4kgs^{-3}). The change of nozzle convergent geometry is more sensitive for the large size nozzle to increase the nozzle damping.

Keywords: nozzle admittance, nozzle damping, combustion instability, linearized Euler equations

PACS® (2010). 47.60.-i

1 Introduction

Combustion instabilities have been frequently observed in solid rocket motors and liquid rocket engines, particularly in the rockets with high design requirement on the performance. Thus, the prediction of combustion instability becomes and for a long time will be a major challenge in the development of rocket motors and engines. However, performing a meaningful stability analysis of a rocket motor or engine is extremely complicate, requiring an evaluation of the energy balance between the various unsteady energy gains and losses, including the pressure-coupled response, the velocity-coupled response, the distributed combustion, the nozzle damping, the particle damping and so on [1]. Among them, the nozzle damping plays the predominant role, as it is usually the largest damping mechanism in rocket motors and engines with longitudinal and mixed transverse/longitudinal modes [2]. Literally, the nozzle damping allows rocket motors and engines to exhaust unsteady energy from the interior. In the past decades, numerous researches have been done to examine the nozzle damping from different aspects, such as the scaling of the nozzle admittance or response [3–5], the determination of the linear nozzle damping coefficient which can then be used for the prediction of overall stability [6, 7], and the nonlinear acoustic behavior of the nozzle and its effect on chamber acoustic modes [5, 8, 9]. After the efforts of decades, the stability models are progressively improved, which in return requires more accurate evaluation of the unsteady energy loss, especially the energy loss through the nozzle damping. Therefore, the method to evaluate the nozzle damping with satisfied accuracy is predominant important and necessary. Furthermore, the nozzle shape is an important consideration in the nozzle design. Because nozzle damping is one of the principle damping mechanisms, the nozzle damping capability and motor stability are sensitive to the change of the nozzle shape [2]. Janardan et al. [10] experimentally concluded that the cavity of the submerged nozzle and the nozzle convergent section geometry have an obvious influence on the nozzle damping capability. However, there are few researches concerning on this subject. In practical application, further investigations are required to help to find effective ways to suppress combustion instability.

The nozzle damping mechanism is closely related to the transformation and transmission process of the perturbation in the nozzle. The perturbation from the unsteady combustion produces the acoustic waves, and when the acoustic waves enter the nozzle, some are reflected back to the chamber, but most are out of the

***Corresponding author: Liu Pei-jin,** Science and Technology on Combustion, Internal Flow and Thermo-Structure Laboratory, Northwestern Polytechnical University, No. 127 West Youyi Road, Beilin District, Xian, China, 710072, E-mail: liupj@nwpu.edu.cn
Wang Mu-xin: E-mail: 15991769681@139.com, **Yang Wen-jing:** E-mail: yangwj@nwpu.edu.cn, **Wei Xiang-geng:** E-mail: realysnow@nwpu.edu.cn, Science and Technology on Combustion, Internal Flow and Thermo-Structure Laboratory, Northwestern Polytechnical University, No. 127 West Youyi Road, Beilin District, Xian, China, 710072

nozzle with the mean flow, as well as the acoustic energy. The acoustic waves can be also generated by the interaction of entropy waves with the accelerated mean flow in the nozzle, which could propagate upstream with the acoustic wave from the chamber and affect the chamber acoustic modes [11]. However, in a real combustion chamber the dissipative effects of turbulence in the mean flow reduce the strength of entropy waves to some extent [12]. Hence the contribution of this process to combustion instability is insignificant, and its evaluation is still controversial. Thus, in this work, only the acoustic waves generated from the combustion are concerned.

Numerous efforts have been dedicated to the analysis of nozzle damping in the past decades. Due to the different flow characteristics between the chamber and the nozzle, to make the analysis simple the nozzle is often considered separately from the chamber, and the acoustic admittance at the nozzle entrance, so called nozzle admittance, is commonly used to characterize the acoustic propagation in the nozzle. Various experiment techniques under the cold-flow condition for measuring the nozzle admittance have been developed, including the direct technique [13], the wave attenuation technique [14], the frequency response technique [14], and the modified impedance tube technique [15],and the modified impedance tube method appears to be the most suitable [16]. Although experiments can provide us the basic understanding of the nozzle admittance and are convenient to deal with complex nozzle designs, to yield enough accurate information about the shape of the standing wave pattern from which the nozzle admittance can be determined, as many pressure measurements as possible at different axial locations along the tube are required, for example 10 examine spots are used in Bell's experiments [15], resulting in an increased amount of data and a large cost. Besides, the experimental errors are inevitable, and in some cases small experimental errors in the measurement parameters can result in large errors in the admittance values [15]. Alternatively, with the fast development of the modeling and the computer technology, the numerical method becomes more and more popular due to its accuracy and low cost. To compute the nozzle admittance is essentially to calculate the acoustic wave propagation in the nozzle. Considering the short, rapidly converging nozzles in solid rocket motors, Crocco [17] considered the case where the length of the nozzle convergent section is much shorter than the wavelength of the oscillation. The nozzle satisfying this condition in general is referred to as being "quasi-steady," and its nozzle admittance is predicted by analyzing the steady-state conservation equations neglecting the influence of the mean flow in the nozzle, known as the short nozzle theory. The short nozzle theory is used widely in the determination of the nozzle damping coefficient in the prediction of combustion instability in solid rocket motors [18]. However, the short nozzle theory always underestimates the nozzle admittance [1], and ignores the effect of the incident wave frequency and the nozzle geometry on the nozzle admittance. To achieve the nozzle admittance calculation with enough accuracy, the influence from the flowfield is worth to deal with caution. Sigman and Zinn [19] described the mean flow in the nozzle through a two dimensional compressible model and used for the following computation of the admittance. The flow field is assumed to be homentropic and non-rotational, and the acoustic velocity potential equation is used to predict the nozzle admittance. The acoustic velocity potential is a versatile parameter that can be used to obtain other acoustic values [6], but it is no longer appropriate to describe the acoustics when dealing with the interaction of acoustic wave and entropy wave in thermoacoustic instability [11]. In summary, compared to the mature experimental techniques for measuring the nozzle admittance, to compute the nozzle admittance, the short nozzle theory is still widely used, which is subjected to strict hypotheses and not accurate enough to meet the requirement of the improved nozzle damping models. For the prediction of combustion instability of engineering level, an accurate and quick method is required to determine the nozzle admittance.

In the present work, the nozzle admittance is predicted using the LEE method taking the effect of the mean flow properties into account. The LEE method is becoming more popular to describe the acoustic wave propagation since viscous contributions are negligible, and it can be extended to modeling the thermoacoustic instability by adding appropriate combustion models. An experimental case [15] is used for the validation of the computational model. Then the damping capability of the nozzle with different geometric parameters is investigated. In the present study, the acoustic energy flux through the nozzle is chosen to evaluate the nozzle damping to simplify computation.

2 Mathematical model

The nozzle is considered finite length and the nozzle admittance is computed by the LEE method. The nozzle damping coefficient is used to evaluate the nozzle damping in most analysis. Morgenweck et al. [20] calculated

both the nozzle damping coefficient and the acoustic energy flux through the nozzle to investigate the attenuation of chamber acoustic modes. Results from the acoustic energy flux are in accordance with the ones from the nozzle damping coefficient. Thus the acoustic energy flux through the nozzle is used to evaluate the nozzle damping.

2.1 Numerical evaluation of nozzle admittance

Nozzle admittance describes the acoustic properties of a nozzle. It is not only the essential parameter in the determination of nozzle damping coefficient, but also the important boundary condition for chamber acoustic modes computation [6, 21]. Here, the following definition of nozzle admittance (Y_e) is used as some previous work [20]:

$$Y_e = \rho_0^* c_0^* \frac{\boldsymbol{u}_1^* \cdot \boldsymbol{n}}{p_1^*} \tag{1}$$

where ρ_0^*, c_0^*, $\boldsymbol{u}_1^*$, and p_1^* are the mean flow density, sound velocity, acoustic velocity and acoustic pressure at the nozzle entrance, respectively.

2.1.1 The LEE method

To establish the mathematical model to calculate the nozzle admittance, several assumptions are adopted:

(1) The nozzle is assumed quasi one-dimensional and only longitudinal waves are considered.
(2) Viscous effects are neglected, and this is consistent with the most acoustic propagation models [22].
(3) Only acoustic waves are considered.

All variables are non-dimensioned through the eq. (2):

$$\boldsymbol{u} = \frac{\boldsymbol{u}^*}{(c_0^*)_s},\ \rho = \frac{\rho^*}{(\rho_0^*)_s},\ p = \frac{p^*}{\gamma(p_0^*)_s},\ t = t^* \frac{(c_0^*)_s}{r_e^*} \tag{2}$$

where $(c_0^*)_s$ is the stagnation sound speed, $(\rho_0^*)_s$ is the stagnation density, $(p_0^*)_s$ is the stagnation pressure, γ is the specific heat ratio, and r_e^* is the nozzle entrance radius.

Then the non-dimensional Euler equations are used, which can help us to find the essential factors affecting the nozzle admittance, and they are generated as:

$$\frac{\partial(\rho S)}{\partial t} + \frac{\partial(\rho \boldsymbol{u} S)}{\partial x} = 0 \tag{3}$$

$$\rho \frac{\partial \boldsymbol{u}}{\partial t} + \rho \boldsymbol{u} \frac{\partial \boldsymbol{u}}{\partial x} = -\frac{\partial p}{\partial x} \tag{4}$$

Following the standard procedure for small perturbation analyses, all variables φ (velocity, pressure or density) are assumed to consist of a mean value $\varphi_0(x)$, which only varies with space, and a small perturbation $\varphi_1(x,t)$, which depends on both space and time:

$$\varphi = \varphi_0(x) + \varphi_1(x,t) \tag{5}$$

For the perturbation, exponential variation in time is assumed:

$$\varphi_1(x,t) = \hat{\varphi}(x) e^{j\omega t} \tag{6}$$

where $\hat{\varphi}$ is the amplitude, and ω is the non-dimensional angular frequency:

$$\omega = \frac{\omega^* r_e^*}{(c_0^*)_s} \tag{7}$$

Introducing eqs (5) and (6) into eqs (3) and (4), the Euler equations are linearized in the frequency domain:

$$\left(\frac{\partial \boldsymbol{u}_0}{\partial x} + \boldsymbol{u}_0 \frac{\partial}{\partial x} + \frac{\boldsymbol{u}_0}{S}\frac{\partial S}{\partial x} + j\omega\right)\hat{\rho} + \left(\frac{\partial \rho_0}{\partial x} + \rho_0 \frac{\partial}{\partial x} + \frac{\rho_0}{S}\frac{\partial S}{\partial x}\right)\hat{\boldsymbol{u}} = 0 \tag{8}$$

$$\left(\frac{1}{\rho_0}\frac{\partial c_0^2}{\partial x} + \frac{\boldsymbol{u}_0}{\rho_0}\frac{\partial \boldsymbol{u}_0}{\partial x} + \frac{c_0^2}{\rho_0}\frac{\partial}{\partial x}\right)\hat{\rho} + \left(\frac{\partial \boldsymbol{u}_0}{\partial x} + \boldsymbol{u}_0 \frac{\partial}{\partial x} + j\omega\right)\hat{\boldsymbol{u}} = 0 \tag{9}$$

2.1.2 The mean flow field

The mean values $\varphi_0(x)$ are determined by the steady solution of eqs (3) and (4). The Mach distribution in the nozzle is obtained by the following the equation:

$$\frac{S(x)}{S_t} = \frac{1}{M_0}\left[\frac{2}{\gamma+1}\left(1 + \frac{\gamma-1}{2}M_0^2\right)\right]^{\frac{\gamma+1}{2(\gamma-1)}} \tag{10}$$

Then the mean pressure and the mean density can be determined with isentropic flow relations:

$$\frac{p_0}{(p_0)_s} = \left(1 + \frac{\gamma-1}{2}M_0^2\right)^{\frac{-\gamma}{\gamma-1}},\ \frac{\rho_0}{(\rho_0)_s} = \left(1 + \frac{\gamma-1}{2}M_0^2\right)^{\frac{-1}{\gamma-1}} \tag{11}$$

The sound velocity of the mean flow c_0 and the mean velocity u_0 are:

$$c_0 = \sqrt{\gamma \frac{p_0}{\rho_0}},\ u_0 = c_0 \times M_0 \tag{12}$$

2.1.3 The numerical resolution

For eqs (8) and (9), the numerical solution method introduced by Lamarque & Poinsot [23] is adopted. In this method, for a given ω, the space is discretized ($x = \{x^{(i)}\}_{1 \le i \le N}$), shown in Figure 1. For chocked nozzles, since the small perturbation cannot travel upstream in supersonic flows, only the convergent section is considered. The finite difference scheme is used for discretization. The mean value $\varphi_0(x)$ and the perturbation $\varphi_1(x,t)$ are discretized as follows (h is the space step):

$$\frac{\partial \varphi_0^{(i)}}{\partial x} = \frac{\varphi_0^{(i-1)} - \varphi_0^{(i+1)}}{2h},\ \frac{\partial \varphi_1^{(i)}}{\partial x} = \frac{\varphi_1^{(i-1)} - \varphi_1^{(i)}}{h} \tag{13}$$

The eqs (8) and (9) can thus be written in a compact form:

$$[A]^{(i)} \begin{pmatrix} \hat{\rho}^{(i)} \\ \hat{\boldsymbol{u}}^{(i)} \end{pmatrix} = [B]^{(i)} \begin{pmatrix} \hat{\rho}^{(i-1)} \\ \hat{\boldsymbol{u}}^{(i-1)} \end{pmatrix} \tag{14}$$

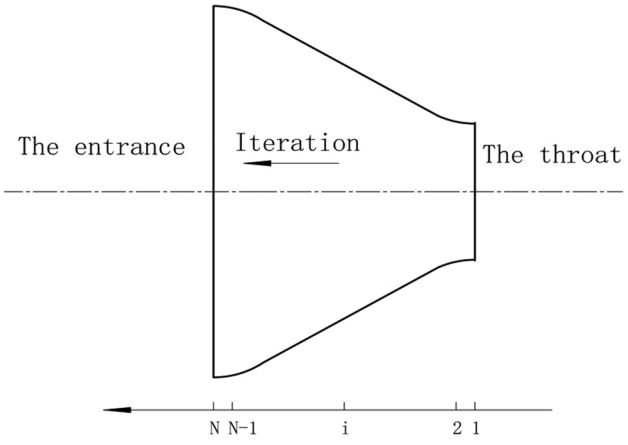

Figure 1: The discretization for computation.

2.1.4 The boundary condition

At the throat, the acoustic wave is not reflected, and the admittance is [24]:

$$Y_t = \frac{(\gamma - 1)\frac{d\boldsymbol{u}_0}{dx} - j\omega}{2\frac{d\boldsymbol{u}_0}{dx} - j\omega} \tag{15}$$

The system (14) can then be iterated from the throat ($x = x$ (1)) to the nozzle entrance ($x = x$ (N)) and the nozzle admittance is obtained.

2.2 Nozzle damping evaluation

In the nozzle, the acoustic energy is lost though the pure acoustic propagation and the convection of the mean flow. The acoustic energy flux ($I_a^\star$) through the nozzle is used to evaluate the nozzle damping, as showing below [20, 25]:

$$\left\langle \boldsymbol{n} \cdot I_a^\star \right\rangle = \frac{1}{T^\star} \int_{t^\star}^{t^\star + T^\star} \boldsymbol{n} \cdot \left[(c_0^\star)^2 \rho_1^\star \boldsymbol{u}_1^\star + \frac{(c_0^\star)^2}{\rho_0^\star} (\rho_1^\star)^2 \boldsymbol{u}_0^\star + (\rho_0^\star \boldsymbol{u}_1^\star + \rho_1^\star \boldsymbol{u}_0^\star)(\boldsymbol{u}_0^\star \cdot \boldsymbol{u}_1^\star) \right] dt^\star \tag{16}$$

A nozzle with a lager acoustic energy flux is expected to have a larger damping capability. Here, the dimensional acoustic energy flux is adopted, and this could clearly show whether the change of nozzle geometric parameters has a great influence on the nozzle damping for a specific nozzle and incident wave frequency range. Introduce the nozzle admittance, and then the acoustic energy flux can be rewritten in the following form:

$$\left\langle \boldsymbol{n} \cdot I_a^\star \right\rangle = \frac{1}{2} \frac{|\hat{p}_e^\star|^2}{\rho_0^\star c_0^\star} \left[\mathrm{Re}(Y_e) + M_0 + M_0 |Y_e|^2 + M_0^2 \mathrm{Re}(Y_e) \right] \tag{17}$$

where $\hat{p}_e^\star$ is the amplitude of the acoustic pressure at the nozzle entrance. $\mathrm{Re}(Y_e)$ in the above equation indicates the acoustic energy loss through the pure acoustic propagation, and the remaining terms are due to the convection of wave energy by the mean flow. It can be seen that the nozzle damping capability mainly depends on the nozzle admittance, especially the real part of nozzle admittance. In the previous studies, it is believed that the real part of the nozzle admittance determines the nozzle damping capabilities, thus the larger real part means the stronger damping capability [19]. However, later we will see that the imaginary part of the nozzle admittance also plays an important role and its effect is included in the term $M_0|Y_e|^2$.

3 Model validation

The nozzle admittance is the essential parameter to evaluate the nozzle damping. The LEE method described

in Section 2.1 eliminates the short nozzle assumption to compute the nozzle admittance used previously, but it is still based on strong assumptions and can only be verified by the comparison with experimental results. Bell [15] performed several experiments to measure the nozzle admittance. The non-dimensional axisymmetric nozzle considered by Bell is shown in Figure 2. Figure 3 shows the correlations between the admittance and the angular frequency from experiments and simulation. In general, the computed values by the LEE method match well with experimental results, and it confirms that the LEE method can predict the nozzle admittance with satisfied accuracy. Only one exception appears around the maximum of the imaginary part of the nozzle admittance in Figure 3 (b). A mathematical model of higher dimensions can offer an improvement in the accuracy of the computed values. Experimental errors may also result in the differences since the two groups of the experimental results also have significant differences.

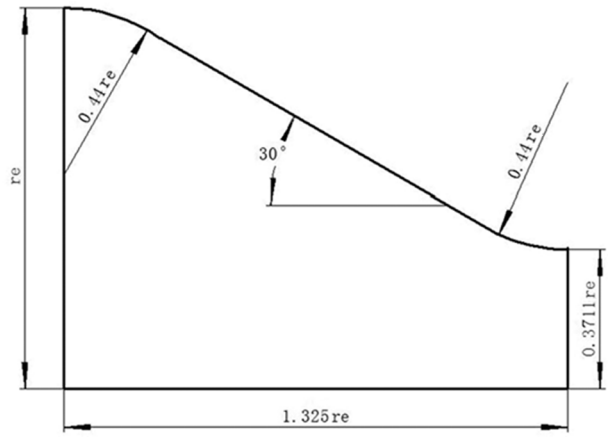

Figure 2: The experimental nozzle configuration [15].

4 Effects of nozzle geometry parameters on nozzle damping

In this section, for a specific choked nozzle, the effects of nozzle geometry parameters on nozzle damping in the intermediate-frequency range (100 Hz–1,000 Hz) are investigated. As mentioned above, the perturbation cannot travel upstream in supersonic flow, thus only nozzle convergent sections are considered. Effects of nozzle convergent geometry, convergent half angle and nozzle size on the nozzle damping are investigated respectively. For each case, the same incident wave at the nozzle entrance is introduced, which means both the frequency and the acoustic pressure amplitude are the same. Then the acoustic energy flux is calculated to evaluate nozzle damping capability. The physical parameters for computation are shown in Table 1.

Table 1: Physical parameters for computation.

Parameters	Values
Mean temperature at the nozzle entrance $(T_0^*)_e$	3,500 K
Mean density at the nozzle entrance $(\rho_0^*)_e$	4 kg/m^3
Specific heat ratio γ	1.18
Acoustic pressure at the nozzle entrance $\hat{p}_e^*$	0.1 Mpa

4.1 Effects of convergent geometry

In this section, the effects of convergent geometry on the nozzle damping are investigated. Three geometries of nozzle, the conical nozzle, concave nozzle and convex nozzle are used, and their configurations are shown in Figure 4. The entrance diameter (de^*), throat diameter (dt^*) are 0.18 m and 0.045 m, respectively. The Mach number at the nozzle entrance is thus 0.0366 according

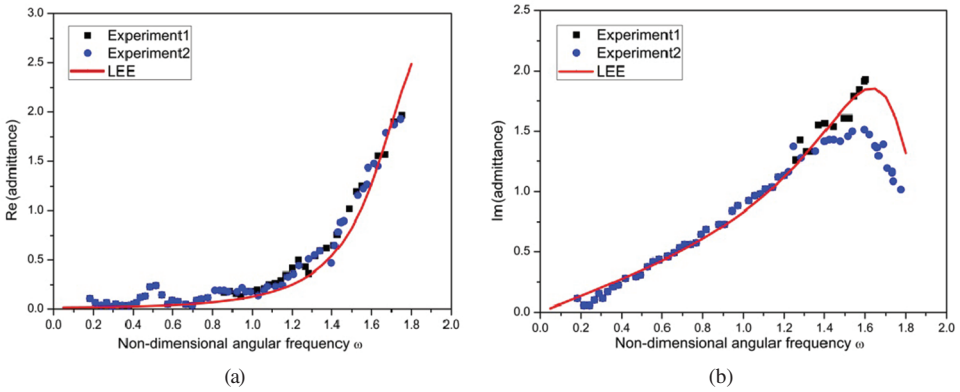

Figure 3: Comparison between the experimental results and computed values. (a) The real part of nozzle admittance; (b) The imaginary part of nozzle admittance.

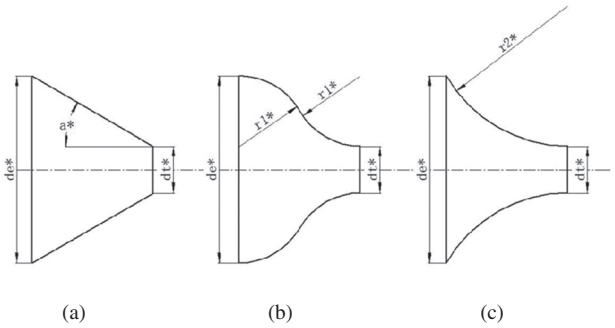

Figure 4: Configurations of three typical geometries. (a) Conical nozzle, (b) Concave nozzle, (c) Convex nozzle.

to the contraction ratio. The convergent length of the three nozzles is the same. For the conical nozzle, its convergent half angle (a^*) is 30°. For the concave nozzle, its converging section is made up of two circular arcs having a smooth transition at the joint. There can be various combinations of the radiuses of the two circular arcs theoretically, and in the present work the radiuses are chosen to be the same and the value ($r1^*$) is 0.0675 m. The convergent section of the convex nozzle is made up of a circular arc and the radius ($r2^*$) can only be 0.135 m since the convergent length is fixed to be same with the other two nozzles.

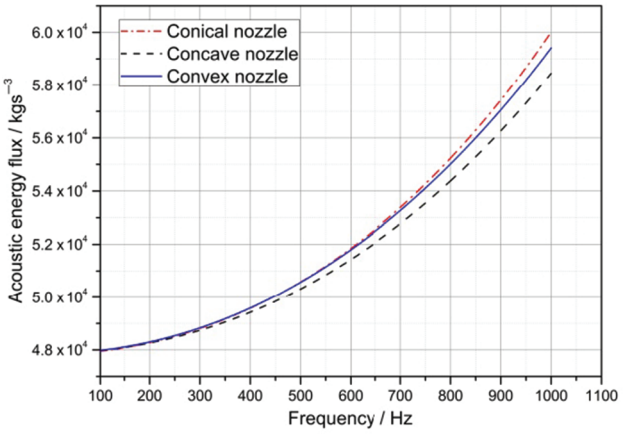

Figure 5: Effects of nozzle geometry on the acoustic energy flux.

Figure 5 shows that with the increasing incident wave frequency more acoustic energy is out of the nozzle, indicating that the nozzle has a stronger damping capability at high frequencies. The conical nozzle always provides the most damping along with the whole frequency range in consideration, which is in accordance with what was found in Janardan's experiments [10]. The difference of the nozzle damping capability is due to the different mean flow properties in the nozzle, which affects the acoustic propagation in the nozzle and then the acoustic energy lost through the nozzle.

The nozzle admittance describes the acoustic propagation in the nozzle and the values of the three nozzles are shown in Figure 6 (a: real part; b: imaginary part). Consisted with the trend of the acoustic energy flux in Figure 5, with the increasing incident wave frequency in the scope of investigation, the nozzle admittances of the three nozzles also increase. It is believed that a nozzle with a larger real part of the nozzle admittance has a stronger damping capability, but our results show that the nozzle with a largest real part of the nozzle admittance does not provide the most damping, indicating the imaginary part of nozzle admittance also plays a non-negligible role. For the conical nozzle, both its real part and imaginary part of the nozzle admittance are relatively high. Thus a large acoustic energy is lost though both the pure acoustic propagation, indicated by the real part of the nozzle admittance, and the convection of the mean flow, affected by both the real part and the imaginary part of the nozzle admittance. For the convex nozzle, though its real part of the nozzle admittance is the largest, its imaginary part of the nozzle admittance is smallest, thus it provides less damping than the conical nozzle. It can be concluded that the real part of the nozzle admittance is considered to dominate the nozzle damping capability, but the imaginary part also shows

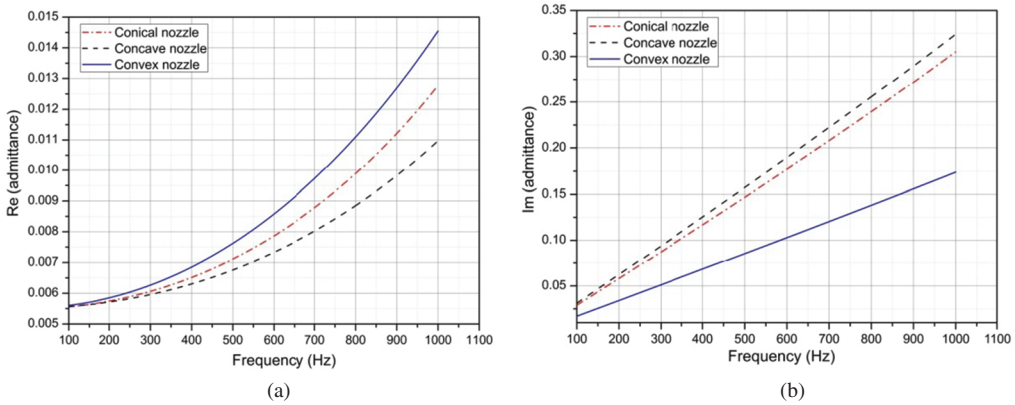

Figure 6: Nozzle admittance of the three nozzles. (a) The real part of nozzle admittance; (b) The imaginary part of nozzle admittance.

the obvious correlation, and its impact depends on the Mach number at the nozzle entrance.

4.2 Effects of convergent half angle

For the conical nozzle, three convergent half angles are adopted, 30°, 45° and 60°, to investigate the effect of convergent half angle on nozzle damping. The entrance diameter and throat diameter are 0.18 m and 0.045 m respectively.

As shown in Figure 7, nozzles still damp acoustic energy more efficiently at high frequencies. The smaller the convergent half angle, the more acoustic energy carried out of the nozzle, which is due to the fact that with the incident wave frequency increasing, both the real part and imaginary part of the nozzle admittance of the nozzle with a smaller convergent half angle increase more rapidly according to Figure 8. The change of convergent half angle essentially leads to the change of nozzle convergent length. It implies that for a fixed contraction ratio, a nozzle with a longer convergent length provides more damping.

4.3 Effects of nozzle size

In Section 3, it is clear that the nozzle admittance varies quickly in high non-dimensional angular frequencies. This includes two basic cases: the incident wave is at a high frequency or the nozzle entrance radius is large. Discussions above show that at high incident wave frequencies, the nozzle provides more damping and the effects of nozzle convergent geometry on nozzle damping are more significant. The entrance radius is a characterization of nozzle size. This section is to study on whether a nozzle of a large size provides more damping and whether its damping capability is more sensitive to the change of nozzle geometry. The conical nozzle, concave nozzle and convex nozzle in Figure 4 are used, but the geometric parameters *de**, *dt**, *r1**, *r2** are 0.36 m, 0.09 m, 0.135 m and 0.27 m, respectively. The convergent half angle is 30°.

According to Figure 9, at a same incident wave frequency, the nozzle of large size dissipates more acoustic energy. Still, the conical nozzle provides the most damping, but the differences among the three nozzles are

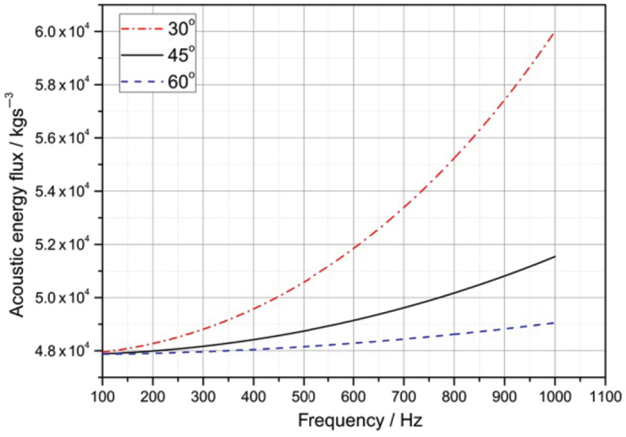

Figure 7: Effects of half convergent angle on acoustic energy flux.

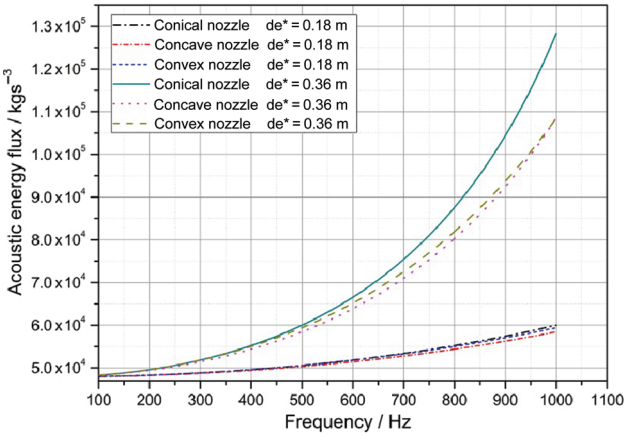

Figure 9: Comparison between the acoustic energy fluxes of nozzles of two sizes.

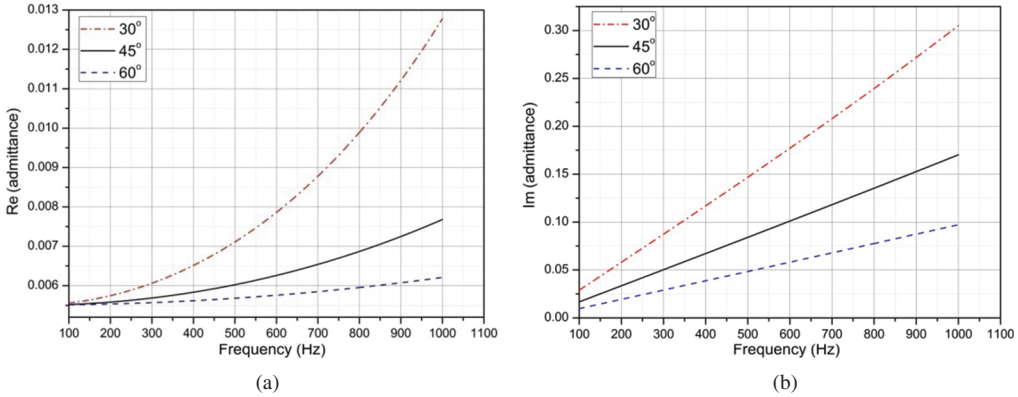

Figure 8: Nozzle admittance of the nozzles with different convergent half angles. (a) The real part of nozzle admittance; (b) The imaginary part of nozzle admittance.

much larger. When the incident wave frequency is 1,000 Hz, for the large size nozzle, the acoustic energy flux through the conical nozzle is 18.3% higher than the concave nozzle, while it is 2.8% for the small size nozzle. This proves that the change of nozzle geometry is more effective for large nozzles to suppress combustion instability.

It should be noted here that in our analysis, we introduced an incident wave that the acoustic pressure amplitude is the same at the nozzle entrance. In a real rocket motor, the incident acoustic wave is determined by the chamber acoustic structure, which depends on the boundary condition at each end, especially the aft end connected to the nozzle defined by the nozzle admittance. For nozzles with different geometries, their nozzle admittances also change and thus the acoustic pressure amplitude at the nozzle entrance may be different. However, for the acoustic modes of low orders which are most concerned, the nozzle admittance has slight effects and the chamber acoustic pressure structures are like the classic acoustic structures of a chamber closed at both ends. Thus, this treatment is reasonable. For acoustic modes of higher orders, to investigate nozzle damping, the accurate chamber acoustic structure needs to be taken into consideration. The value of acoustic pressure amplitude also has no effects on the conclusions in the linear regime.

5 Conclusions

The nozzle admittance is computed by the LEE method taking the mean flow properties into consideration, which allows investigating the effects of the incident wave frequency and the nozzle geometry on the nozzle admittance and the nozzle damping. The computed values by LEE are consistent with the experimental results. Then the acoustic energy flux through the nozzle is calculated to estimate the damping characteristics of nozzles with different geometries. It is shown that the imaginary part of the nozzle admittance plays a non-negligible role in the determination of the nozzle damping. Among the conical, concave and convex nozzle, the conical nozzle always provides the most damping. With the increasing convergence half angle, the nozzle damping capability significantly decreases. Nozzles of bigger sizes damp acoustic energy more efficiently and are also more sensitive to the change of nozzle geometry. This proves that the change of nozzle geometry is more effective for large nozzles to suppress combustion instability.

Acknowledgements: This study was presented at APCATS 2015 (www.apcats2015.or.kr).

Funding: Project 51206136 supported by National Natural Science Foundation of China.

Nomenclature

a	convergent half angle
$[A]$	complex matrix
$[B]$	real matrix
c	sound velocity, m/s
d	the diameter, m
f	the incident wave frequency, Hz
j	$\sqrt{-1}$
h	space step, m
I_a	acoustic energy flux, kgs^{-3}
Im	the imaginary part
M	Mach number
N	number of discretization nodes
$\boldsymbol{n}$	normal surface vector
p	pressure, Pa
Re	the real part
$r1$	radius of the concave nozzle, m
$r2$	radius of the convex nozzle, m
r	the radius, m
T	period of oscillation, s
t	time, s
$\boldsymbol{u}$	velocity, m/s
x	space coordinate
Y	admittance
φ	variables
ρ	density, kg/m^3
γ	specific heat ratio
ω	angular frequency, rad/s
$\langle\rangle$	time averaging of one period

Superscripts

*	= dimensional values
^	= amplitude

Subscripts

0	= mean values
1	= perturbation values
e	= at the nozzle entrance
s	= stagnation values
t	= at the nozzle throat

References

1. Zinn BT. Nozzle damping in solid rocket instabilities. AIAA J 1973;11:1492–7. DOI:10.2514/3.50616.
2. Blomshield FS. Lessons learned in solid rocket combustion instability. 43rd AIAA/ASME/SAE/ASEE Joint Propulsion Conference & Exhibit, AIAApaper2007-5803, Cincinnati, OH, July 2007.

3. Crocco L, Sirignano WA. Behavior of supercritical nozzles under three-dimensional oscillatory conditions, AGARD-OGRAPH-117, 1967.
4. Janardan BA, Daniel BR, Zinn BT. Scaling of rocket nozzle admittances. AIAA J 1975;13:918–23. DOI:10.2514/3.60470.
5. Moase WH, Brear MJ, Manzie C. The forced response of chocked nozzles and supersonic diffusers. J Fluid Mech 2007;585:281–304. DOI: 10.1017/S0022112007006647.
6. French JC. Nozzle acoustic dynamics and stability modeling. J Propul Power 2011;27:1266–75. DOI:10.2514/1.B34239.
7. Javed A, Chakraborty D. Damping coefficient prediction of solid rocket motor nozzle using computational fluid dynamics. J Propul Power 2014;30:19–23. DOI:10.2514/1.B35010.
8. Padmanabhan MS. The effect of nozzle nonlinearities on the nonlinear stability of liquid rocket motors. Ph.D. Thesis, School of Aerospace Engineering, Georgia Institute of Technology, Atlanta, Georgia, 1975.
9. Moase WH, Brear MJ, Manzie C. Linear and nonlinear acoustic behavior of outlet nozzles.15th Australasian Fluid Mechanics Conference, the university of Sydney, Australia, December 2004.
10. Janardan BA, Daniel BR, Zinn BT. Effect of nozzle design parameters upon attenuation of axial instabilities in solid rockets. 9th AIAA/SAE Propulsion Conference & Exhibit, AIAApaper1973-1223, Las Vegas, Nevada, November, 1973.
11. Nicoud F, Wieczorek K. About the zero Mach number assumption in the calculation of thermoacoustic instabilities. Int J Spray Combust Dynamics 2009;1:67–111. DOI:10.1260/175682709788083335.
12. Sattelmayer T. Influence of the combustor aerodynamics on combustion instabilities from equivalence ratio fluctuations. J Eng Gas Turbines Power 2003;125:11–19. DOI: 10.1115/1.1365159.
13. Crocco L, Monti R, Grey J. Verification of nozzle admittance theory by direct measurement of the admittance parameter. Ars J 1961;31:771–5. DOI: 10.2514/8.5627.
14. Bufflun RG, Dehority GL, Slates R, Price EW. Acoustic attenuation experiments on subscale cold flow rocket motors. AIAA J 1967;5:272–29. DOI:10.2514/3.3952.
15. Bell WA. Experimental determination of three-dimensional liquid rocket nozzle admittances. Ph.D. Thesis, School of Aerospace Engineering, Georgia Institute of Technology, Atlanta, Georgia, 1972.
16. Culick FEC, Dehority GL. Analysis of axial acoustic waves in a cold flow rocket. J Spacecraft Rockets 1968;6:591–5. DOI:10.2514/3.29618.
17. Crocco L, Sirignano WA. Effect of transverse velocity components on the nonlinear behavior of short nozzles. AIAA J 1966;4:1428–30. doi:10.2514/3.3691.
18. Flandro GA, Majdalani J. Aeroacoustic instability in rockets. AIAA J 2003;41:485–97. doi:10.2514/2.1971.
19. Sigman R, Zinn BT. Theoretical determination of nozzle admittances using a finite element approach, 18th Aerospace Sciences Meeting, AIAA paper 80–0085, Pasadena, California, January 1980.
20. Morgenweck D, Sattelmayer T, Fassl F, Kaess R. Influence of scaling rules on the loss of acoustic energy. J Spacecraft Rockets 2011;48:498–506. DOI:10.2514/1.48334.
21. Nicoud F, Benoit L, Sensiau C, Poinsot T. Acoustic modes in combustors with complex impedances and multidimensional active flames. AIAA J 2007;45:426–41. DOI:10.2514/1.24933.
22. Duran I, Moreau S. Solution of the quasi-one-dimensional linearized Euler equations using flow invariants and the magnus expansion. J Fluid Mech 2013;723:190–231. DOI:10.1017/jfm.2013.118.
23. Lamarque N, Poinsot T. Boundary conditions for acoustic eigenmodes computation in gas turbine combustion chambers. AIAA J 2008;46:2282–92. DOI:10.2514/1.35388.
24. Lieuwen TC, Yang V. Combustion instabilities in gas turbine engines: operational experience, fundamental mechanisms and modeling, Progress in Astronautics and Aeronautics, 210, AIAA, Reston, VA, 2005.
25. Jacob EJ. A study of nonlinear combustion instability. Ph.D. Thesis., University of Tennessee, Knoxville, 2009.